CHAPTER III

THE TELESCOPE PERFORMANCE

1. Introduction

In this chapter we shall review the various factors which determine how well the telescope may be expected to perform. The results of this review then permit estimates to be made of the way the instrument can be used under various climatic conditions.

2. The Dynamic Behavior of the Telescope Structure

As has been said already in the section on the drive and control system, the ability to point the telescope and its performance in winds depend on its structural dynamics. Thus, the structural design was made with the intent that it should have both good static behavior (i.e., it should satisfy the conditions for homology and strength) and also good dynamic behavior. The analysis of its dynamics could only be made when the design was reasonably complete; in this section we describe the dynamic analysis and give its results.

(a) The dynamic analysis requirements. The structure is massive and elastic. It can obviously vibrate in a wide variety of oscillatory modes at various natural frequencies. The fact that there will be quite low damping associated with such oscillations is clear from simple principles--steel at normal working stresses shows very small elastic loss and welded joints are similarly behaved. Losses can be expected to exist in the air damping of the structure, in the gears of the drive gear-boxes and in the movement of the ground under the concrete foundation, but these effects are small.

The dynamic analysis must identify the main oscillatory modes, particularly those at the lowest natural frequencies. This emphasis on the low-frequency modes arises from the fact that wind turbulence is mainly effective in exciting the lowest frequencies. For a structure of this size both theory and experiment show that energy exchange from the

wind to the structure begins to fall in importance at about 0.02 Hz and drops rapidly above about 0.3 Hz. The lowest structural natural frequency should be well above these values; experience says that it should be about 1.5 Hz and this value was the target chosen during the design.

In addition to the large-scale or body-vibrational modes, it is important to consider possible vibrational modes in individual components of the structure. Most of these are at high frequencies, weakly coupled to the total structure and are of no importance. The vibrations of individual members may, however, be important. In Chapter II, Section 4, we have discussed the possibility that wind-induced vibrations (due to von Karman vortices) could affect the survival of the tubular members, and we have concluded that this is safely avoided. Nevertheless, the method of dynamic analysis of the structure must also recognize and allow for the existence of vibrations in the long tower members since these might reduce the lowest system resonances; the present analysis does this.

(b) The method of dynamic analysis (SDL Report H-10, Chapter 9, Simpson, Gumpertz & Heger Report No. 9333) The analysis was conducted in two stages. First, the reflector structure was treated. The reflector, feed support legs and elevation wheel, including the applied masses of the surface and the observing cabins, were analyzed to determine the dynamic characteristics as seen by the elevation bearings. The results of this detailed analysis, which was made by Simpson, Gumpertz & Heger, can be represented by treating the whole reflector as a body with fixed mass and fixed moments of inertia supported by infinitely stiff bearing and drive points. This mass-inertia system was then associated with six degrees of freedom, each of which had a particular stiffness. This dynamical equivalent to the reflector was then applied to the tower and the second stage of the analysis, the inclusion of the tower stiffness and inertia, was made. The result was the modes of oscillation of the combined tower-reflector system.

The analysis of the tower proceeded as follows. The tower structure was modeled assuming its individual members to be pin-jointed at their ends but with appropriate masses and equivalent member stiffnesses concentrated at the member centers and also (to allow for the heavy joints) with masses at the joints themselves. This model reproduced the natural oscillatory modes of the tower, including the effects of individual members. There are further equivalent springs in such a system; bearings, gears, the azimuth trucks and rail and even the concrete foundation all contribute springs to the system, and appropriate values were supplied for these quantities.

With this input, a digital computer structural dynamics program, developed by the Space and Re-entry Systems Division of the Philco-Ford Corporation at Palo Alto, was used to make the dynamic analysis. Two reflector positions were used, when it was pointing towards the zenith

and also at 45° from the zenith. This latter position is known to be close to the situation which gives the lowest natural frequency for the structure.

The analysis was tested for sensitivity to various parameters. For example, it was rerun with the values of reflector mass and inertia increased first by 10 percent and then by 20 percent. A similar pair of runs was made with the stiffnesses reduced by 10 percent and 20 percent. A run in which the tower structure joints were rigid rather than pinned was made and the solution shown to be insensitive to this change.

(c) The results. The dynamic analysis of the reflector alone was carried out with two sets of boundary conditions; for each of the two the elevation bearings were taken as fixed points. In the first analysis, joint No. 58 was taken as fixed as far as tangential gear movements were concerned, and in the second analysis joint No. 54 was similarly treated. These two conditions well-describe the telescope in the zenith and at 45° from the zenith. One analysis was performed with antisymmetric conditions along the (x,z) plane. (See Figure 26 for the coordinate system.) The results of these analyses showed the first ten possible vibration modes. The lowest frequency revealed was 2.56 Hz and the mode with this frequency was the simple rotation of the reflector about the x-axis. The simple rotation mode of the reflector about the elevation axis (the y-axis) had frequencies of 2.87 Hz (zenith position) and 2.68 Hz (45° position). For full details see the Simpson, Gumpertz & Heger Report No. 9333.

These reflector results, when combined with the tower structure, trucks, gears and foundations, showed the dynamic modes for the whole telescope. The six modes having the lowest natural frequencies are sketched in Figure 26 and are described in words in the following Table 10. The first reflector modes already described are included in the table as modes Nos. 5 and 6, although these are modes of the reflector only and not of the whole structure. It should be realized that modes 3 and 5 are coupled, so are modes 2 and 6; the frequencies given for modes 2 and 3 include the effects of these couplings.

3. The Accuracy of the Homologous Performance

(a) The sources of variation (S. von Hoerner Report No. 33). Although in principle the solution to the problem of obtaining truly homologous behavior of the reflector support structure should be limited only by the computational accuracy of the computer, in practice there will be a number of causes contributing to a less-than-perfect deflection pattern for the reflector surface. In this section we examine these causes and calculate their effects on the resulting accuracy of the reflector surface. The actual reflector structure will deviate

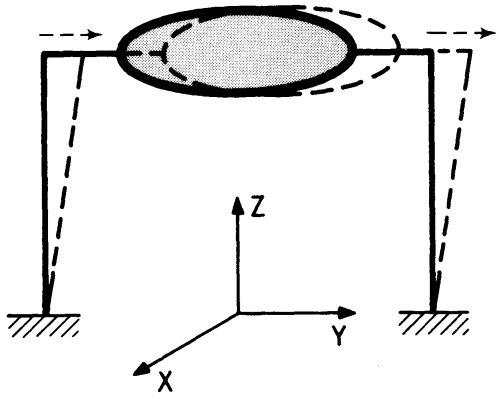

MODE 1

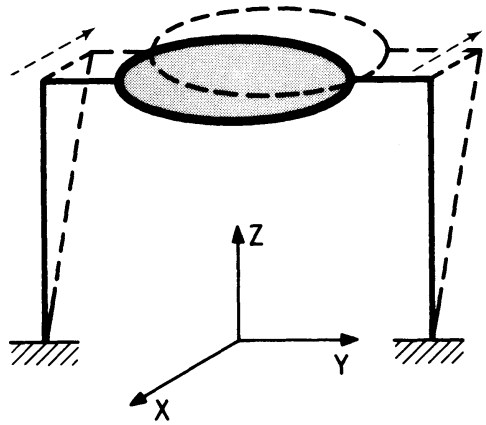

MODE 2

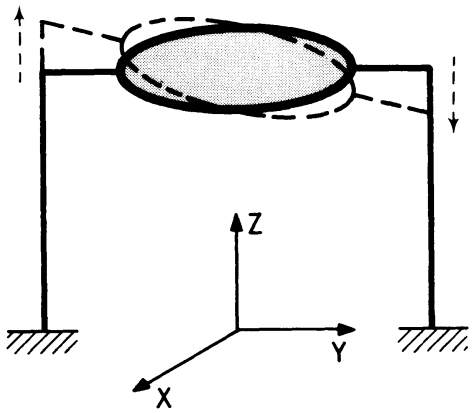

MODE 3

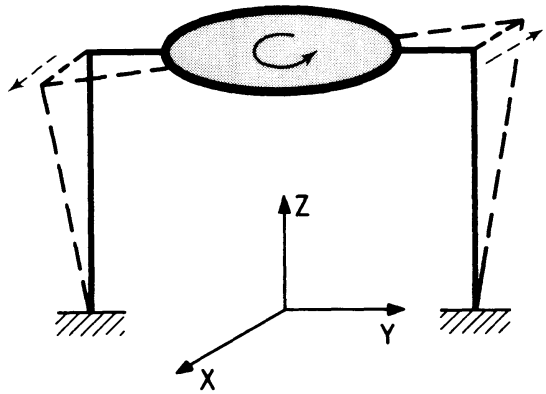

MODE 4

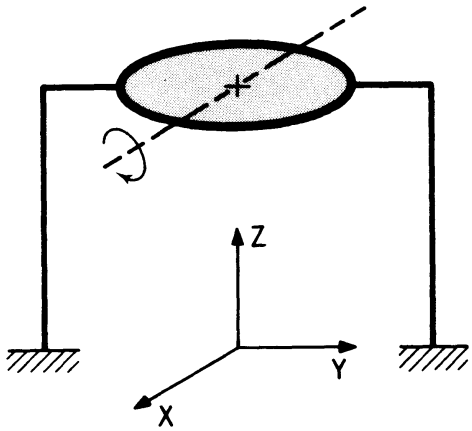

MODE 5

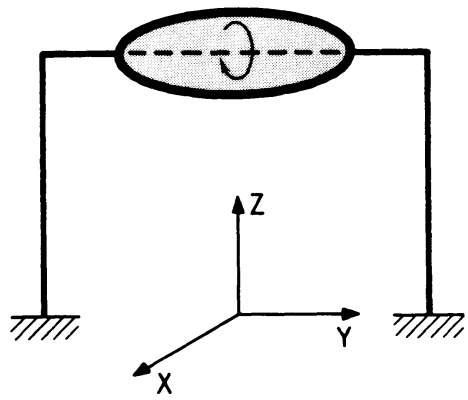

MODE 6

Figure 26. The main modes of oscillation of the telescope.

Table 10. Six Main Modes of Oscillation of the Telescope

Mode No.	Description	Frequency* for Reflector Position Zenith	45°
1.	The tower tops rock backward and forward along the line of the elevation axis	1.61±0.05 Hz	1.52±0.06 Hz
2.	The tower tops rock together in phase along the line perpendicular to the elevation axis and approximately parallel to the ground.	1.92±0.04 Hz	1.61±0.06 Hz
3.	The tower tops rock one up, one down in antiphase in the vertical direction.	2.31±0.11 Hz	1.67±0.07 Hz
4.	The tower tops rock in antiphase, otherwise as in Mode 2. This mode rotates the reflector about the vertical azimuth axis.	2.44±0.01 Hz	2.00±0.05 Hz
5.	Rotation of the reflector about an axis perpendicular to the elevation axis and parallel to the reflector aperture.	2.56 Hz	2.56 Hz
6.	Rotation of the reflector about the elevation axis.	2.87 Hz	2.68 Hz

*The ± values correspond approximately to the range of values when the reflector stiffness or inertia is changed by 10 percent.

from the structure developed by the homology program for the following reasons:

(i) The members used to build the telescope will have bar areas which differ somewhat from the design area. This will arise because as many members as possible will be made from commercially available pipes or tubes, and the bar areas of these will not be exactly correct. Also, for these members and for the members which are specially made, fabrication tolerance will cause stiffness differences.

(ii) The spherical joints add weight to the structure. They also replace small lengths of the member ends and thus modify the total stiffness of any given member.

(iii) The linear dimensions of the structure as built will differ slightly from the design dimensions. This in turn means a departure from homology since both the geometry and the member stiffness change somewhat.

(iv) Forces can be applied to the reflector structure from other parts of the telescope as it moves. For example, lack of perfect level of the azimuth track can apply forces from the tops of the towers to the elevation bearings.

There are other effects which might cause departures from homology; variations of Young's modulus or of thermal expansion coefficient between various members might occur. Such effects are, however, small for run-of-the-mill steel of good commercial quality.

(b) Expected variations in bar areas (S. von Hoerner Report No. 33, W-Y. Wong Report No. 34(A). Most of the reflector support structure members are steel tubes or pipes, with areas of cross-section between 0.5 sq. inch up to 16 sq. inches. In choosing these members, various criteria have to be met. Adequate radius of gyration to avoid buckling must be supplied by giving an adequate length/radius ratio. The wall thickness must be sufficient to allow of easy welding, yet below 0.4 inches to keep thermal lag small. The frequency of any wind induced vibrations must be kept above about 2.5 Hz and fatigue must be avoided by either avoiding vibration or keeping the alternating stress small enough.

When all these requirements are met, it is found that most of the members can be supplied by using tubes or pipes which are of standard manufacture. Some, however, must be specially fabricated from steel plate by rolling and welding. For all types of member, the departures of the actual bar areas from the required area were found. Departures of about 1 percent were permitted in selecting members from the suppliers' lists. Manufacturing tolerances were found to be about 5 percent in most instances, although in a very few cases it may be necessary to select actual pipes or tubes to keep the area tolerances below 5 percent.

With this information it is then possible to estimate the total expected RMS departure from the design bar area, and, as Report No. 33 shows, this average departure will be on the average 2.3 percent of the bar area.

(c) Variations in weight and stiffness of the joints. The homology calculations give the stiffnesses of members connecting the points where the members intersect. In the practical structure, these points are the centers of the spherical joints and the members are shorter than the distance between these points by the sizes of the joints. The effects of the joints on the homology solution is thus to replace a short

length of the member; this in turn changes the weight and the stiffness of the member by small amounts, and then the homology condition is no longer exactly satisfied.

In the first design of the joints the condition was imposed that the change in weight due to the joints (the difference between the joint weights and the weights of the member lengths no longer needed) should be no more than about 5 percent of the total structure weight. Similarly, it was planned that the average percentage stiffness change should be less than about 3 percent. These figures were chosen with a reasonable knowledge of what their effects on homology might be.

The first design process for the joints could not produce a detailed optimum design for each joint; this task remains to be done in the detailed design of the telescope. Thus the changes in weight and stiffness which result from the first design can be regarded as upper limits, capable of some further improvement.

The changes may be described as follows:

(i) The weight of each of the reflector structure members is changed. The average change in weight, expressed as a percentage of the member weight, is $\overline{\Delta W}$.

(ii) The individual values ΔW for the members deviate randomly about $\overline{\Delta W}$; this deviation is described by the RMS value of $(\Delta W - \overline{\Delta W})$, and expressed as a percentage.

(iii) The stiffness of each member changes and as for the weights, the average stiffness change $\overline{\Delta K}$ is expressed as a percentage of K and the deviation of the stiffnesses from $\overline{\Delta K}$ is described by the RMS value of $(\Delta K - \overline{\Delta K})$ expressed as a percentage.

The average weight and stiffness changes, and the individual variations about these average values both contribute to departures from homology.

The first joint design resulted in the following values:

$$\overline{\Delta W} = +2.5\% \qquad \text{RMS } (\Delta W - \overline{\Delta W}) = \pm 2.0\%$$

$$\overline{\Delta K} = -3\% \qquad \text{RMS } (\Delta K - \overline{\Delta K}) = \pm 2.0\%$$

(d) Dimensional accuracy and azimuth track irregularity. The reflector structure must be built to a good, but not excessive, dimensional accuracy. We specify that this accuracy, expressed as the RMS deviation of each of these three coordinates of a point on the structure from its required position, should be 0.25 inch (6.4 mm). This specification will require a well-controlled erection procedure; for example, dimensional errors in the reflector structure should be reasonably random and should not develop any large-scale consistent pattern.

Undulations in the azimuth tracks will be the chief source of distorting forces applied to the reflector structure. The specifications for this (including truck, rail and foundation distortions under working loads) suggest that the maximum vertical movement of the tower bases will result in a lateral force on the reflector structure at the elevation bearings of 50 tons.

(e) Estimates of the effects on the reflector surface. In order to estimate the total departures from homology due to all the above effects, the following set of computations was made. Three representative reflector support structures were chosen, each of which showed good homologous performance (ΔH_o, the RMS deviation of the surface points, from a true paraboloid, was small). Changes were then made to each of these structures in separate runs for each of the quantities whose effect on homology was to be found. The changes were introduced as random numbers with their mean values and deviations equal to the desired amounts. The structures, so modified, were then reanalyzed and the new departures from homology (ΔH_c) was found. The additional deviation

$$\Delta H = \left\{(\Delta H_c)^2 - (\Delta H_o)^2\right\}^{1/2}$$

was calculated. In all, 16 such experimental calculations were performed. The results are summarized in the following Table 11.

(f) Discussion. The total RSS departure from homology is thus seen to be acceptably small. It should be noted that items 1-6 in the table all depend on the elevation angle (i.e., the value of ΔH is that corresponding to a movement of the telescope from zenith to horizon) and therefore could, if so desired, be still further reduced if the telescope surface were set (say) at 30° from the zenith and used mainly over the zenith to 60° depression angle range. (See Report No. 33 for further discussion.) However, no such reduction in ΔH is made before using ΔH in the telescope error budget (Chapter III, Section 5).

4. Effects of Wind and Temperature on the Telescope Performance

(a) Introduction. The most serious effects on the performance of the telescope arise from the influence of wind and of temperature differences and changes on various members of the structure. Both these influences bend and deflect the structure. Note that it is differences of temperature and fairly rapid changes of temperature with time which degrade accuracy. When all the telescope is at the same temperature, its performance is not degraded.

The telescope loses accuracy for both these causes in two ways. First, the reflector surface departs from its true shape, and thus

Table 11. The Deviations from Homology

Change Applied to the Structure	Resulting ΔH	
	inches	mm
1. None -- the value of ΔH for the "perfect" homology solution	0.002	0.051
2. Apply the average $\overline{\Delta W}$ = +2.5% $\overline{\Delta K}$ = -3% for the spherical joints	0.0012	0.030
3. Apply the deviation in stiffness due to joints RMS ($\Delta K - \overline{\Delta K}$) = ± 2%	0.0017	0.044
4. Apply the deviation in weight due to joints RMS ($\Delta W - \overline{\Delta W}$) = ± 2%	0.0017	0.043
5. Use standard pipes, include fabrication tolerances of bar areas ΔA = ± 2.3%	0.002	0.051
6. Permit xy and z coordinates of points to vary ± 0.25 inch	0.0013	0.033
7. Permit a track irregularity of ± 0.25 inches	0.0009	0.023
RSS value of ΔH	0.0042	0.107

becomes less efficient at short wavelengths. Second, the ability to point the radio beam of the telescope is degraded since wind and temperature differences can deflect the radio beam without causing the positioning mechanism to sense and correct these beam deflections. We shall call these two effects (i) degradation of surface accuracy and (ii) degradation of pointing accuracy and in this section describe the magnitudes of the effects.

(b) Permissible magnitudes. Ideally, neither loss of surface accuracy nor of pointing accuracy is permissible. However, we have adopted throughout the criteria that the following can be permitted and still result in a satisfactory instrument at its shortest operating wavelength:

(i) The RMS surface accuracy may, in total, be degraded to $\lambda_{min}/16$ (λ_{min} is the shortest usable wavelength).

(ii) The RMS precision for tracking may be degraded to one-fifth of the HPBW at λ_{min}. (HPBW is the half-power beamwidth.)

These criteria represent a significant departure from perfection. The $\lambda_{min}/16$ surface accuracy results (if the deviations are random) in a gain reduction of the instrument to a value of 0.54 of its full gain for a perfect reflector. In practice this means that the aperture efficiency would drop from about 60 percent (perfect reflector) to 32 percent at λ_{min} with the imperfect reflector. The tracking precision of one-fifth of the HPBW implies that the signal from the source would be reduced by a factor of 0.90 when the beam is at its 1σ deviation from the true direction.

It is generally accepted that "perfect" performance for a radio telescope results when the surface accuracy is $\lambda_{min}/32$ and the tracking accuracy is one-tenth the HPBW at λ_{min}. The gain loss factors then are 0.86 (for surface irregularity) and 0.97 (for pointing).

(c) Temperature effects (Report No. 37, S. von Hoerner and V. Herrero). Although effects of temperature and wind will act together on the telescope, it is convenient to discuss them separately. Two main questions have to be answered in describing the temperature effects. (1) What temperature differences are likely to be experienced by the structure? (2) What will the effects of these be on the surface and pointing accuracies?

The first question is best answered by experience and experiment. The telescope structure will be painted with a well-tested thermal control paint. This has been used on all NRAO telescopes and on the Goldstone 210-foot, as well as on many others. It has high reflectivity in the visible light range, yet radiates well in the long infrared. Thus, direct heating by sunlight is reduced and yet any temperature differences can radiate themselves away.

(i) Measurements of temperature differences and changes: A series of measurements has been made on the NRAO telescopes (particularly the 140-foot, a spare 140-foot panel, the 36-foot on Kitt Peak, and on one 85-foot), and on a test surface plate for the present telescope. Study of work by JPL on the Goldstone telescope confirms the nature and magnitude of the results; so also do measurements and calculations of the temperature changes in typical components of the telescope structure. These measurements are discussed and analyzed in S. von Hoerner and V. Herrero's Report No. 37 in some detail.

The quantities whose values are needed may be summarized as follows. We are chiefly concerned with the magnitudes of the effects on clear, calm, sunny days and on clear, calm (or nearly calm) nights, since these conditons demonstrate the most and least severe effects of temperature

on performance. Temperature differences existing vertically across the structure are the largest in practice and thus the most important. They are referred to here as $\Delta T°$ F. Since telescope members of different sizes respond differently with time to changes of temperature (i.e., their thermal lag is different), we need also to know the values of dT/dt or $\dot{T}$ (degrees F per hour) where T is the ambient air temperature. In deriving the values for ΔT and $\dot{T}$ to be used in the thermal analysis from observations, the 95 percent level of the distributions of ΔT and $\dot{T}$ were used--this means that the calculated thermal deformations will be greater than the actual deformations for 95 percent of the time.

The results of measurements of ΔT and $\dot{T}$ are listed in the following Table 12. From this the further Table 13 was derived, giving the values to be adopted for the thermal deflection analysis.

(ii) The thermal deflection analysis. This analysis must be carried out for all the important parts of the structure carried on the elevation bearings. The reference platform pointing system removes from consideration thermal effects on the tower. The thermal effects on the panels and on the support structure were analyzed by computation. The effect of ΔT on a surface plate (NRAO type) was measured. A test plate was adjusted while at a uniform temperature and then exposed outside on a clear day. The temperature difference between its upper surface and a rib behind the surface was measured. The contour of the surface was measured (at 37 points) when ΔT was $-6.95°$ F and again when ΔT was $+2.10°$ F. (This change occurred as the plate came out of the shadow of a building into full sun.) From these measurements the expected contributions to the RMS surface accuracy could be calculated. They are shown in Table 14 of Section 5.

The analysis of the panel structure was straightforward. Both ΔT and $\dot{T}$ have to be considered although the thermal lag contribution is in fact small except at dawn and dusk. The analysis was made in the computer by assigning changed lengths to members in accordance with the temperature regime. The chief thermal effect is a degradation of the surface accuracy; there is only a small contribution to the pointing accuracy errors. The results of the analysis are given in Tables 14 and 15 of Section 5.

The support structure analysis was made by computing the deformations of the surface points and of the subreflector support legs under the various thermal loads. The results here are both a loss of pointing accuracy and the degradation of surface accuracy. A part of this surface accuracy degradation is due to the support structure deformation, but a part also comes from the movement of the subreflector; both effects are combined to give the total surface degradation.

The thermal analysis, when applied to the support structure, shows that the main contributions to the pointing errors come from temperature differences between the subreflector support legs. The detailed design

Table 12: Summary of Measurements of ΔT and $\dot{T}$ on Various Structures (95% level)

Description of Measurement	Applicable to:	ΔT °F		$\dot{T}$ °F/hour	
		Clear Night	Noon Sun	Clear Night	After Sunset
ΔT measured on 140-foot spare panel	Surface panels		14.0		
$\dot{T}$ for 1 year at Sugar Grove	Panels, structure				8.5
Heavy members of 140-foot corrected for lag	Panels, structure		12.0		
Tower members and legs of 85-1 telescope at Green Bank	Structure		5.4		
140-foot reflector support structure	Panels, structure	2.2			
Surface to support structure of 36-foot on Kitt Peak	Surface, panels, structure		12.5		
Surface to support structure on 36-foot on Kitt Peak	Surface, panels, structure	1.9			
Test surface plate for 65-meter telescope at Green Bank	Surface	2.0	9.2	1.5	8.6

Table 13. Values for ΔT and $\dot{T}$ Adopted for the Thermal Deflection Analysis

Component part of the 65-meter Telescope	Adopted Values			
	ΔT °F		$\dot{T}$ °F/hour	
	Clear Night	Noon Sun	Clear Night	After Sunset
Reflector surface plates	2.0	12.0	1.5	8.6
Panels	1.5	9.0	1.5	8.6
Reflector support structure	1.5	9.0	1.5	8.6

and analysis of the subreflector support legs is given in Report No. 42 by W-Y. Wong. Since the most critical requirements arise at the shortest wavelengths, where the telescope will be operated with Cassegrain optics, this is the case which is analyzed in detail. The results show that temperature differences between the legs are very important. If there is a 1° F temperature difference randomly distributed between the four legs of the feed support, the RMS contribution to the pointing error is 2.0 arc seconds.

It can thus be concluded that the main contribution to pointing error due to structural temperature differences arises from the legs which support the subreflector (the feed-support legs). The changes of length of these legs both rotates and translates the subreflector and it is these motions which primarily affect the pointing.

(d) Wind effects (S. von Hoerner and V. Herrero, Report No. 39. The use of a stable reference platform mounted at the axes intersection removes from consideration a number of the effects of wind on the telescope. The following effects, however, remain and their magnitude has been determined.

(i) Steady or irregular winds will distort the reflector. This will degrade the reflector surface accuracy and will introduce pointing errors.

(ii) Steady or irregular winds will deflect the subreflector support legs. This results mainly in pointing errors but may also cause a gain reduction due to the displacement of the subreflector from its required position with respect to the surface and to the feed system.

(iii) Irregular winds will produce torques about both telescope axes. Although, in principle, the servo system used in the azimuth and elevation drives can sense the pointing errors due to these imposed torques, and can thus correct them, this is only true for disturbances

whose frequencies fall within the range where the servo system is operative. The remaining pointing errors due to the higher-frequency gusts still remain.

To evaluate these effects due to wind, properties of the wind itself and its spatial and temporal structure have to be known. In addition to quite extensive information in the literature, a lengthy set of observations were made at Green Bank on a tower 150 feet high to confirm that the figures used in the wind analysis were satisfactory. Report No. 39 by S. von Hoerner and V. Herrero summarizes the wind information which has been used in the analysis and also gives the calculations of the wind-induced deformations of the telescope structure (excluding the feed-support legs). Report No. 42 by W-Y. Wong studies the wind deformations of the feed support legs. The assumptions and calculations made of these effects have been checked by having independent studies made by Simpson, Gumpertz & Heger. In discussing the wind-induced pointing errors due to the drive system, the results of SDL Report No. H-10 are used.

We now summarize the results of these various studies.

(i) Effects of wind on the reflector structure. Various pressure distributions which arise from wind forces on the reflector have been analyzed. The reflector surface was divided into a number of areas, one for each of the surface joints where the panels are held, and the force due to the wind pressure acting on the area was concentrated at the joint.

The joint displacements were then computed and a program determined the best fitting paraboloid and computed: (a) RMS surface error. (b) Defocussing gain losses expressed as an equivalent RMS surface error. (c) The total equivalent surface error resulting from (a) and (b). (d) The angular pointing error.

The results of this analysis for a wind mean speed of 18 miles per hour showed that the contribution to the RMS surface error was 0.076 mm and the average contribution to the pointing error was 3.2 arc seconds.

(ii) Effects of wind on the feed support legs. The principal effect here is the pointing error which results from the wind on the feed legs and focal point cabin producing a lateral displacement of the subreflector. (As in the case of temperature effects, the Cassegrain mode is the one most likely to suffer from these effects.) The analysis (W-Y. Wong Report No. 42) shows that an 18 miles per hour wind produces a pointing error of 1.1 arc seconds.

(iii) The effects of wind on the performance of the drive and control system. Wind acting on the antenna will cause errors in the servo-controlled pointing system, since the wind can produce varying torques on the structure about both the azimuth and the elevation axes. To counteract these torques the servo drive must develop a position error signal at its input. When the rate of fluctuation of the wind torque is

slow enough, compared to the response of the servo, these position errors are corrected. The servo response (its gain as a function of frequency) must, however, be limited at higher frequencies since the drive must not be able to give energy to the structure at any frequencies approaching the dynamical resonances of the structure. Thus, if there are wind torques with components in this frequency range outside the servo response, they will produce pointing errors. The spectrum of wind torques acting on large antennas is quite well established, both from direct measurement and from calculations based on wind structure. Thus, when the servo response is known, the positional errors can be calculated. Two such calculations are made in SDL Report No. H-10 (Chapter 11.7) and show that, at 18 miles per hour, the RMS position error due to this effect is 0.4 arc seconds.

(e) Summary. All these effects are summarized in the following Section 5 in the form of surface accuracy and tracking error budgets. The thermal and wind effects provide limitations to the telescope performance which are about the same in magnitude as other limitations; from this it may be concluded that the design is roughly balanced; i.e., all the various possible limitations appear to have about the same magnitude for a telescope of this size.

5. The Surface and Tracking Accuracy Budgets

(a) General. The two most important quantities on which the telescope performance depends are the overall reflector surface accuracy (including the subreflector) and the pointing precision. In this section we summarize the various contributions to these two quantities in the form of error budgets. In such a budget, it is usually conservatively correct to assume that the various contributions are mutually independent, and thus to add them by taking the root of the sum of the squares (RSS) of the individual contributions.

We express the surface accuracy by taking the root mean square (RMS) value of the departures of many approximately equally spaced surface points from a true parabolic surface. We choose for this reference surface that paraboloid which best fits the surface points; its focal length, axis direction and vertex position are permitted to vary. We do not, however, as is sometimes done, weight the points according to the illumination pattern of the reflector.

We measure pointing accuracy by the quantity which is often called tracking accuracy, and define it as follows. We assume that the telescope has been well-calibrated over all the useful sky insofar as its repeatable pointing errors are concerned. We then set it to track a point which is moving in the sky at about the sidereal rate. (At the equator and on the meridian this is a rate of 15 minutes of arc per

minute of time.) The RMS value of the angular departures of the center of the telescope beam from its required position in the sky is the tracking accuracy, and it is measured in seconds of arc.

As has already been discussed in Section 4 of this chapter, the telescope will be considered as performing satisfactorily at its shortest wavelength λ_{min} if:

$$\text{surface accuracy} = \lambda_{min}/16$$

$$\text{tracking accuracy} = 1/5 \text{ (half-power beamwidth at } \lambda_{min})$$

(b) The reflector surface accuracy. In the following three-part table are listed the various factors which contribute to the overall surface accuracy. We have separated those factors which do not depend on wind or on temperature, and given references to the sections of this report where the magnitudes of the quantities are discussed in more detail.

Table 14. The Telescope Surface Accuracy Error Budget

(i) The surface accuracy under conditions of no wind and constant uniform temperature.

Table 14(i)

Source of Error	Reference to this Report	Magnitude (1σ value)
Departure of main reflector structure from true homologous behavior	Chapter III, Section 3	$\pm$ 0.004 inch $\pm$ 0.107 mm
Departures of panels from true homologous behaviour	Chapter II, Section 4	$\pm$ 0.002 inch $\pm$ 0.051 mm
Fabrication tolerances of individual surface plates	Chapter II, Section 5	$\pm$ 0.003 inch $\pm$ 0.076 mm
Gravitational deflections of individual surface plates	Chapter II, Section 5	$\pm$ 0.0014 inch $\pm$ 0.035 mm
Setting accuracy of the surface plates on the telescope	Chapter II, Section 5	$\pm$ 0.0049 inch $\pm$ 0.125 mm
Total subreflector surface errors (fabrication and gravitational)	Chapter II, Section 6	$\pm$ 0.002 inch $\pm$ 0.051 mm

The RSS of the last column = ± 0.0080 inch or 0.200 mm.

(ii) The effect of wind on the surface accuracy. The following additional errors result from a gusty wind of 18 miles per hour mean speed at the level of the reflector center.

Table 14(ii)

Source of Error	Reference to this Report	Magnitude (1σ value)
Total surface errors due to wind on reflector structure, including equivalent error due to reflector defocussing	Chapter III, Section 4	± 0.0029 inch ± 0.076 mm
Effect of wind deforming the panel structure	Chapter II, Section 4	± 0.0008 inch ± 0.020 mm
Effect of wind deforming the surface plates	Chapter II, Section 5	± 0.006 inch ± 0.015 mm
Effect of wind on sub-reflector support, including tilting, and lateral transition--translated to equivalent surface error	Chapter II, Section 6	± 0.0002 inch ± 0.005 mm

RSS of last column = 0.0032 inch or 0.080 mm.

(iii) The effect of structural temperature differences and changes on the surface accuracy. Two temperature regimes are chosen for display here; in both these the telescope performance depends on (1) the vertical structural temperature difference ΔT and on (2) the rate of change of ambient temperature with time, $\dot{T}$. Table 14(iii) gives the contributions to the surface error corresponding to various ΔT and $\dot{T}$ values. The values chosen are typical for a sunny day, and will only be exceeded on 5 percent of all clear nights. (See Section 4 of this Chapter for more details.)

(c) The telescope tracking accuracy error budget. The following three-part Table 15 summarizes the tracking accuracy, first under the conditions of no wind and uniform constant temperature; then wind and temperature effects are added.

Table 14(iii)

Source of Error	Temperature Regime	Error Magnitude (1σ)	Combined Error (1σ)
Reflector support structure	Clear sunny day ΔT = 9.0° F $\dot{T}$ = 8.6° F/hour	± 0.0123 inch ± 0.31 mm	
Panel structure	Clear sunny day ΔT = 9.0° F $\dot{T}$ = 8.6° F/hour	± 0.0056 inch ± 0.14 mm	± 0.0169 inch ± 0.430 mm
Surface plates	Clear sunny day ΔT = 12.0° F $\dot{T}$ = 8.6° F/hour	± 0.0102 inch ± 0.26 mm	
Reflector support structure	Clear night ΔT = 1.5° F $\dot{T}$ = 1.5° F/hour	± 0.0021 inch ± 0.054 mm	
Panel structure	Clear night ΔT = 1.5° F $\dot{T}$ = 1.5° F/hour	± 0.0009 inch ± 0.020 mm	± 0.0028 inch ± 0.072 mm
Surface plates	Clear night ΔT = 2.0° F $\dot{T}$ = 1.5° F/hour	± 0.0017 inch ± 0.043 mm	

Table 15. The Telescope Tracking Accuracy Error Budget

(i) The tracking accuracy with no wind and uniform constant temperature.

Table 15(i)

Source of Error	Reference to this Report	RMS Error (1σ) arc second
Drive and Control System	Chapter II, Section 8	0.9
Hysteresis and limit cycling errors.		
Tracking and acceleration errors.		0.6
Stable Reference Platform System	Chapter II, Section 7	
Platform hysteresis and encoder errors		1.0
Autocollimator errors		0.9
Atmospheric effects on light beams		0.6
System noise		0.5

RSS of last column = 1.9 arc seconds.

(ii) The tracking accuracy in the presence of wind. The following additional errors arise in the presence of gusting wind of average speed 18 miles per hour at the reflector center.

Table 15(ii)

Source of Error	Reference in this Report	RMS Error (1σ) arc second
Disturbance to drive, control and position reference system.	Chapter II, Section 8	0.4
Deflections of reflector support structure due to steady and gusting wind components.	Chapter III, Section 4	3.2
Deformations of panel and surface plates.	Chapter III, Section 4	0.3
Deflections of subreflector support system.	Chapter II, Section 6	1.1

RSS of last column = 3.4 arc seconds.

(iii) The tracking accuracy in the presence of temperature differences and changes. The temperature regimes corresponding to a clear, sunny day and a clear night are again used in this table.

Table 15(iii)

Source of Error	Temperature Regime	Error Magnitude (1σ) arc seconds	Combined Error (1σ) arc seconds
Reflector support structure	Clear sunny day ΔT = 9.0° F $\dot{T}$ = 1.5° F/hour	2.4	
Panel structure and surface plates	Clear sunny day ΔT = 9.0° F $\dot{T}$ = 1.5° F/hour	Negligible	8.5
Subreflector support system	Clear sunny day ΔT between legs = 4° F $\dot{T}$ = 1.5° F/hour	8.2	
Reflector support structure	Clear night ΔT = 1.5° F $\dot{T}$ = 1.5° F/hour	0.40	
Panel structure and surface plates	Clear night ΔT = 1.5° F $\dot{T}$ = 1.5° F/hour	Negligible	1.1
Subreflector support system	Clear night ΔT between legs = 0.5° F $\dot{T}$ = 1.5° F/hour	1.0	

6. The Estimated Performance of the Telescope Under Various Climatic Conditions

(a) The effects of the atmosphere on radio astronomical observations at millimeter wavelengths. The main atmospheric effects on observations are the absorption of radio waves in the atmosphere and the radiation from the warm and wet atmosphere of radio noise into the radio telescope radiometer. A possible further effect is that lack of uniformity in a horizontal plane in the refractive index of the atmosphere can cause phase irregularities on the incoming wave front and thus reduce the effective gain of the instrument. (The refraction of the uniform atmosphere is important, but it does not degrade performance. It can be allowed for by measuring at ground level the atmospheric temperature, pressure and relative humidity.)

(i) Atmospheric absorption. Figure 27 shows typical values for the absorption of radio waves passing once vertically down through the atmosphere. The main contributions come from oxygen and water vapor; of these the water vapor contribution is the variable. Two water-vapor curves are shown, one for a dry atmosphere (W_v = 3.4 mm) and one for a rather humid atmosphere (W_v = 21 mm). (W_v is the total precipitable water in the whole atmospheric depth, i.e., if all the water vapor in a vertical column were liquified it would have a depth of W_v.)

Figure 27 shows that good ground-based millimeter wave observations can be made in and near the atmospheric windows. It also explains why the present telescope is planned to work up to 86 GHz, so as to take advantage of the window there. The dry atmosphere has an absorption of about 8 percent at 86 GHz at the zenith, and observations are not seriously influenced by such absorption. It should perhaps be noted that Figure 27 cannot be interpreted as saying that no work can be done outside the windows. Spectral-line observations are often possible close to the absorption lines; for example, the CO line at 115.27 GHz (λ = 2.6 mm) lies close to the oxygen absorption peak at 118.75 GHz, yet it has been easily observed with the NRAO 36-foot telescope.

(ii) Atmospheric noise. Radiated noise from the atmosphere can be troublesome at all wavelengths shorter than about 10 cm. However, under clear sky and dry air conditions millimeter-wave observations have been made with good precision. This subject is considered in more detail in Chapter IV on the site for the telescope.

(iii) Irregular refraction. The effects of irregular atmospheric refraction on the gain and pointing precision of large reflector telescopes at millimeter waves are not yet directly known, but there is good evidence from interferometer measurements and some other observations that these effects will not limit the performance of the present instrument (See Findlay 1971).

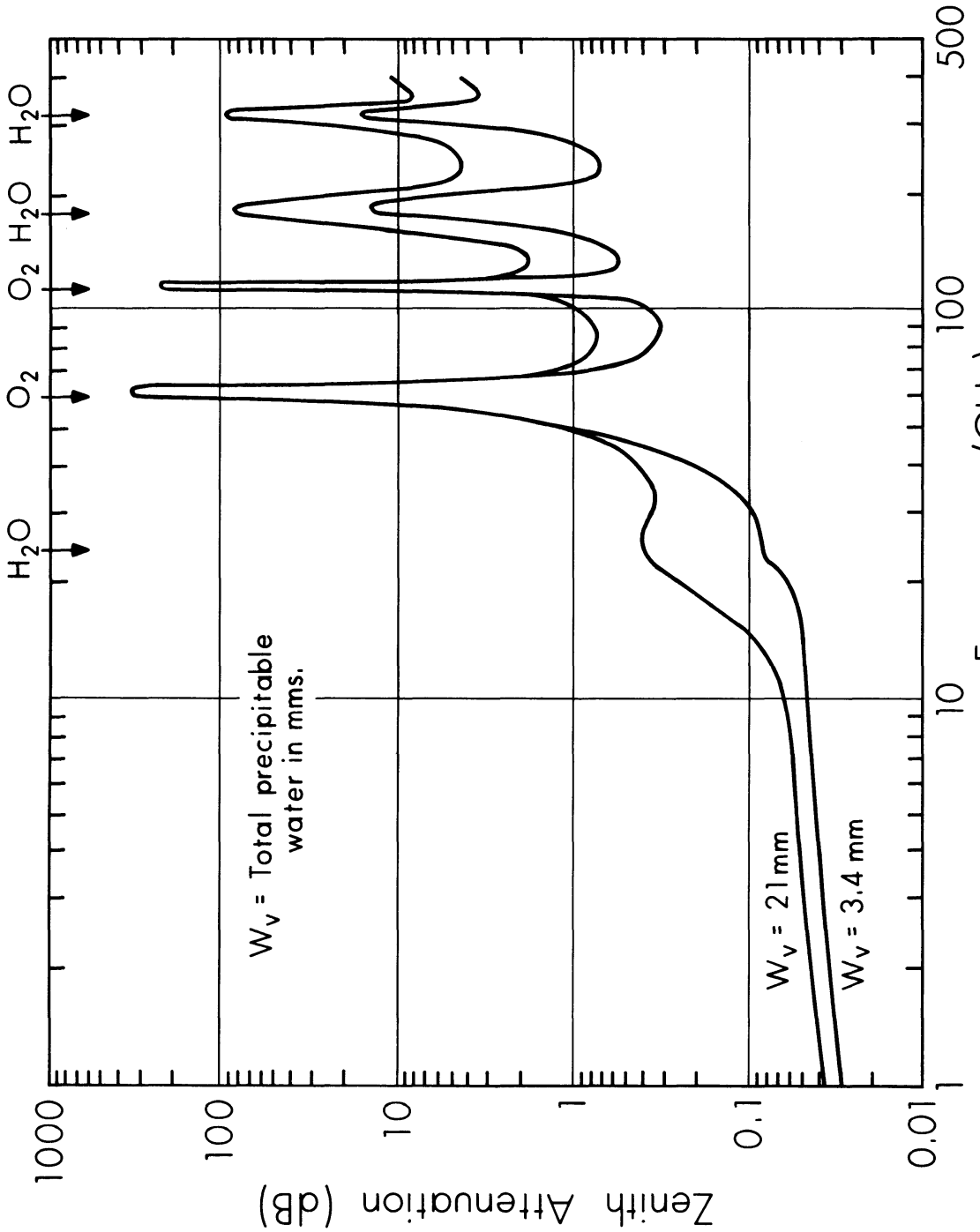

Figure 27. One-way zenith absorption of radio waves in the atmosphere.

(b) Performance under various climatic conditions. Let us summarize the information in the error budgets of Tables 14 and 15, and attempt to show how the telescope will perform under some typical atmospheric conditions. We will discuss, as a measure of its performance, the shortwave limit of the telescope λ_{min}. This limit is set either because the reflector surface accuracy deteriorates or because the tracking accuracy deteriorates. We continue to use the criteria:

$$\lambda_{min} = 16 \times \text{RMS Surface Accuracy}$$

or

$$\text{HPBW at } \lambda_{min} = 5 \times \text{Tracking Accuracy.}$$

We now attempt to collect the values of surface and tracking accuracy under various weather conditions. The sunny day and clear night cases have been discussed, so has the effect of a steady wind. When we try to estimate what will happen when wind and temperature effects are combined, the problem becomes more difficult. In Report No. 36 von Hoerner has attempted to estimate how the combination affects accuracy insofar as the reflector surface is concerned. He made temperature measurements on the surface and on a supporting rib of the NRAO surface plate under conditions of a flow of air across the plate. Two air velocities were used, and for the plates he derived an expression for Δz, the deformation of the surface plates:

$$\Delta z \text{ in full sunshine} = \frac{8.3 \times 10^{-3}}{1+v/3.8} \text{ inches} \qquad \text{III(1)}$$

$$\Delta z \text{ at night} = \frac{1.8 \times 10^{-3}}{1+v/3.8} \text{ inches} \qquad \text{III(2)}$$

where v = wind speed in miles/hour.

If we can assume the same form for the variation of temperature effects with wind, we can compile the following expressions:

(i) Surface accuracy with wind acting--clear night and sunny day. The contributions to the surface accuracy budget are:

$\pm$ 0.200 mm (Table 14(i) -- no wind or temperature)

$\pm$ 0.080 $(v/18)^2$ mm (Table 14(ii) -- assuming contribution varies as v^2)

$\pm \frac{0.072}{1+v/3.8}$ mm (Table 14(iii) -- for a clear night)

or

$$\pm \frac{0.430}{1+v/3.8} \text{ mm (Table 14(iii) -- for a sunny day).}$$

(ii) Tracking accuracy with wind acting--clear night and sunny day. The contributions to the tracking accuracy budget are:

$\pm$ 1.9 arc seconds (Table 15(i) -- no wind or temperature).

$\pm$ 3.4 $(v/18)^2$ arc seconds (Table 15(ii) -- assuming contribution varies as v^2)

$$\pm \frac{1.1}{1+v/3.8} \text{ arc seconds (Table 15(iii) -- clear night)}$$

or

$$\pm \frac{8.5}{1+v/3.8} \text{ arc seconds (Table 15(iv) -- sunny day)}$$

We can now use the error contributions (by forming the RSS values) to arrive at Table 16, which estimates the telescope performance under various conditions.

(c) Conclusion. We must stress that the simple methods used to mix the effects of wind and temperature to arrive at Table 16 can only give a rough answer. We believe, however, that the estimates of performance with the climatic factors unmixed are reasonably good.

The telescope will be at its best on clear nights when a wind of a few miles per hour is blowing. Under such conditions its RMS surface accuracy is $\lambda/16$ for a wavelength of 3.2 mm and its tracking accuracy is 2.15 arc seconds, which is 1/7 of the HPBW of the telescope at 3.2 mm wavelength.

At its worst (with no wind on a sunny day) it will work at 9 mm wavelength (33 GHz).

7. The Performance of Some Other Telescopes

(a) General. The present 65-meter telescope will not be the largest fully-steerable reflector in the world, but when its size is considered together with its planned shortwave performance, it becomes an instrument some steps ahead of all others in its requirements for accuracy. Thus it is not possible by considering existing instruments and their performance to give full experimental evidence from these telescopes that the 65-meter will work as well as planned. Nevertheless, there are a number of experimental facts about the measured performance of existing telescopes which give some support to the calculations and predictions made in this Report. We will in this section list these facts, again emphasizing that they, in themselves, are not advanced as proof of the 65-meter design.

The quantities which are of greatest interest are the surface and tracking accuracies (as already defined in Chapter III, Section 5), and

Table 16. Performance of the Telescope Under Various Climatic Conditions

	Wind Velocity Miles/Hour	Surface Accuracy (1σ) mm	Tracking Accuracy (1σ) arc seconds	λ_{min} (mm)		λ_{min} mm (GHz)
				Surface	Tracking	
Clear Night	0	0.215	3.2	3.45	2.35	3.45 mm (87)
	6	0.200	2.0	3.20	2.15	3.20 mm (94)
	12	0.205	2.4	3.30	2.55	3.30 min (91)
	18	0.215	3.9	3.45	4.20	4.20 mm (71)
Sunny Day	0	0.475	8.7	7.60	9.30	9.30 mm (32)
	6	0.260	3.8	4.15	4.05	4.15 mm (72)
	12	0.230	3.1	3.70	3.30	3.70 mm (81)
	18	0.230	4.2	3.70	4.50	4.50 mm (67)

we concentrate on measurements of these for existing telescopes. Surface accuracy can be measured by high-class surveying, but also, once a telescope is working, it can be determined by using antenna tolerance theory (Ruze 1966). Results of the two methods agree well. Tracking and pointing accuracy can also be measured, since by now a number of small diameter radio sources are known in absolute position to errors of rather less than one arc second. The actual measurements, however, represent not only the errors in the radio telescope but also errors introduced because the noise power received from the source is often only one or two orders of magnitude more than the radiometer noise fluctuations. This causes errors in position measurements, whose magnitude depend on the telescope beamwidth and on the signal/noise ratio in the observations. Also, measures of tracking accuracy also include any irregular atmospheric refraction which is added to the telescope errors. With these restrictions in mind, we list experimental information from a number of telescopes.

(b) The 210-foot Goldstone telescope. This instrument, built by the Rohr Corporation for the Jet Propulsion Laboratory, is of particular interest since it is a well-designed and well-built telescope of the size we are describing (210 feet is 64 meters). The telescope has been working as part of the Deep Space Instrumental Facility since 1966; a considerable number of radio astronomers have used it and the antenna group at JPL and others have made many careful measurements of its performance. Information about the 210-foot has been most useful in the present design, but the single important fact to note here is its excellent tracking performance.

To measure this, the telescope was set to track a strong radio source, but with the source not in the center of the telescope beam but on the side of the beam. In this situation, small angular tracking errors show up as signal level changes, and after a simple calibration and calculation the result can be used to measure the angular tracking accuracy. In one such experiment (Bathker 1969) the 1σ RMS tracking accuracy was measured to be 3.6 arc seconds. This is an extremely good result and considerably exceeds the original telescope specification. It is relevant to the 65-meter, since the dynamical properties and servo design parameters of our telescope and the JPL telescope are similar, but ours has, of course, a much higher angular resolution in its encoders.

(c) The 210-foot Parkes telescope. This is one of the oldest large fully-steerable telescopes; it was built at a low cost with the intention of its working well at 21-cm wavelength. In fact it has been used down to 5 cm and the central 100 feet has been tested at 22 GHz (1.4 cm) and shown to have useful gain. This telescope has good tracking accuracy, as is demonstrated by a long series of observations of positions of 750 radio sources (CSIRO staff 1969) where the RMS (1σ) source positions were found to 10 arc seconds in RA and 12 arc seconds in declination. The observations were made at night, but include read-out

errors and errors due to radiometer noise, so they show that the telescope behaves well over the significant periods of time between the source and calibration source observations.

(d) The NRAO 300-foot transit telescope. The NRAO 300-foot telescope was not built with any expectation of high positional accuracy, but since its resurfacing and subsequent use at shorter wavelengths it has been possible to measure its pointing performance. Two reports by M. M. Davis (September 14 and October 25, 1971) give the RMS pointing errors as follows. (These errors are the RMS departures in position from the telescope calibration curve and so are equivalent to what we have called tracking errors for the 65-meter telescope.)

Table 17. Pointing Errors of the NRAO 300-foot Telescope

Type of Observation	RMS Angular Error (1σ)
Elevation measurements Day and Night	± 9 arc seconds
Right ascension measurements	
Daytime (mainly sunny)	± 9.7 arc seconds
Nighttime	± 2.1 are seconds

It should be noted that all the observations contain the errors due to radiometer noise and the elevation measurements include the read-out errors (the digit interval on the encoders is 10 arc seconds). The RA measurements show clearly the effects of sunshine and show also excellent structural stability at night. In particular, they give good support to our 65-meter tracking error estimates insofar as they confirm structural integrity and repeatability at night. They also demonstrate that critical items, such as the feed support, do not on the average experience troublesome temperature differences at night.

(e) The NRAO 36-foot telescope. This telescope has, or course, proved itself to be the most useful millimeter-wave instrument in the world. It is used in an astrodome, but the 40-foot wide dome opening does in fact expose the telescope to some wind and temperature effects during observations. Its RMS tracking accuracy is 5 arc seconds, including radiometer noise and read-out errors (the 1 bit angular encoder interval is 1.24 arc seconds). The RMS surface accuracy is 0.005 inches (0.144 mm) as determined from an aperture efficiency of 50 percent at 85 GHz.

(f) Other millimeter-wave telescopes (Findlay 1971). The following table shows the tracking and surface accuracies of some other telescopes.

Table 18. Tracking and Surface Accuracies of Some Other Telescopes

Property	USSR Crimean RT-22	Aerospace Corp.	U. Texas	U. Calif., Berkeley
Diameter in meters	22.0	4.57	4.87	6.10
Tracking accuracy in arc seconds	9.0	7.2	7.2	9.6
RMS surface accuracy in mm	0.12	0.05	0.10	0.15

(g) Conclusion. This brief survey confirms that, although the 65-meter telescope is an instrument of higher performance than any so far built, there is supporting experimental evidence to show that the tracking and surface accuracies expected of it are not too advanced over those already achieved in some other telescopes.

References

Bathker, D. A. 1969, Radio Frequency Performance of a 210-foot Ground Antenna: X-Band, JPL Technical Report 32-1417, Jet Propulsion Laboratory, Pasadena, California.

CSIRO Staff 1969, Aust. J. Phys. Astrophys. Suppl. No. 7.

Findlay, J. W. 1971, Annual Review Astron. and Astrophys., 9, 271-292.

Ruze, J. 1966, Proc. Inst. Elec. and Electronics Engrs., 54, 633-640.